BIOCHEMISTRY
including biophysical chemistry & molecular biology

Article

pubs.acs.org/biochemistry

# von Willebrand Factor Antagonizes Nitric Oxide Synthase To Promote Insulin Resistance during Hypoxia

Bandana Singh,[†] Indranil Biswas,[†] Iti Garg,[†] Ragumani Sugadev,[‡] Abhay K. Singh,[§] Sharmistha Dey,[§] and Gausal A. Khan*,[†]

[†]Department of Physiology, Defence Institute of Physiology and Allied Sciences, Lucknow Road, Timarpur, New Delhi 110054, India

[‡]Department of Bioinformatics, Defence Institute of Physiology and Allied Sciences, Lucknow Road, Timarpur, New Delhi 110054, India

[§]Department of Biophysics, All India Institute of Medical Sciences, Ansari Nagar, New Delhi 110029, India

Supporting Information

**ABSTRACT:** Hypoxic respiratory diseases or hypoxia exposures are frequently accompanied by glucose intolerance and impaired nitric oxide (NO) availability. However, the molecular mechanism responsible for impaired NO production and insulin resistance (IR) during hypoxia remains obscure. In this study, we investigated the possible mechanism of impaired NO production and IR during hypoxia in a mouse model. Mice were exposed to hypoxia for different periods of time (0−24 h), and parameters of IR and endothelial dysfunctions were analyzed. Exposure to hypoxia resulted in a time-dependent increase in IR as well as multimeric forms of von Willebrand factor (vWF) and subsequently a decrease in eNOS activity. Preincubation with plasma of hypoxia-exposed animals (different time points) or human vWF inhibited insulin-induced NO production in a dose-dependent manner; larger doses of insulin reversed the effect. In contrast, preincubation of vWF-immunodepleted plasma failed to inhibit insulin-induced NO production, whereas vWF immunoneutralization abolished the effect of hypoxia-induced IR and D-[U-$^{14}$C]glucose uptake. Furthermore, the interactions between vWF and eNOS were studied by far-Western blotting, co-immunoprecipitation, and surface plasma resonance spectroscopy. Kinetic analyses showed that the dissociation constant ($K_D$), inhibitory constant ($K_i$), and half-maximal inhibitory concentration ($IC_{50}$) were $1.79 \times 10^{-8}$ M, 250 pM, and 18.31 pM, respectively, suggesting that vWF binds to eNOS with a high affinity and greater efficacy for activator (insulin) inhibition. These results indicated that vWF, an antagonist of eNOS, inhibits insulin-induced NO production and causes IR.

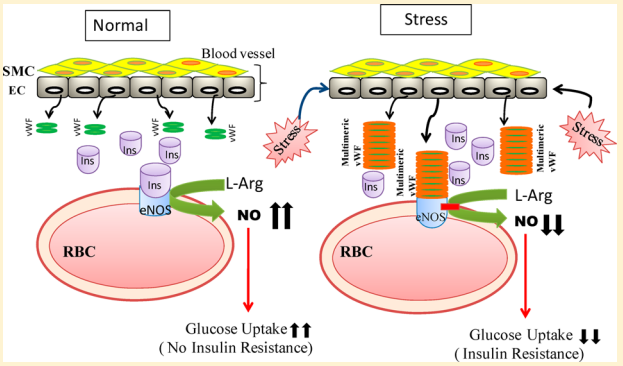


Glucose intolerance is a basic clinical feature of the metabolic syndrome whose growing prevalence has led to an increase in cardiovascular morbidity and mortality in industrial countries. In respiratory diseases such as chronic pulmonary disease (CPD) or obstructive sleep apnea (OSA) and altitude hypoxia, glucose intolerance is frequently observed. Obesity is the main risk factor for glucose intolerance and diabetes mellitus, but CPD or OSA is associated with glucose intolerance that is independent of the body mass index and mainly caused by hypoxia.[1,2] The prevalence of CPD and OSA is high and both diseases are increasingly linked to cardiovascular diseases (CVDs).[3] The association between insulin resistance (IR), CVDs, and hypoxia also seen in high-altitude exposure, hypoxic gas breathing, or hypobaria has been reported previously in both human and animal models.[1,4,5] Exposure to altitude hypoxia elicits changes in glucose homeostasis, with an increase in glucose and insulin concentrations within a few days.[4]

Insulin induces vasodilatation by modulating endothelial nitric oxide synthase (eNOS) activity and expression through activation of the insulin receptor/insulin receptor substrate-1/2 and phosphatidylinositol 3-kinase/protein kinase B/Akt signaling cascade.[6−8]

Deficiency of NO is believed to be the primary defect that links endothelial dysfunction (ED) and IR in hypoxia.[9,10] The production of NO plays an important role in preventing vascular diseases via the regulation of thrombosis, vascular tone, and remodeling.[11] The treatment of human erythrocytes, platelets, and neutrophils with insulin stimulated the synthesis of NO through activation of a membrane-bound constitutive form of insulin-activated nitric oxide synthase.[12,13] NO is an endothelium-derived relaxing factor. It is a chemically unstable compound with a half-life of 3−5 ms in an aqueous solution. It activates guanylate cyclase in various cells, including platelets, and has also been shown to be a second messenger of insulin.[14,15] The reduced bioavailability of NO is thought to be one of the

**Received:** January 8, 2013
**Revised:** December 12, 2013
**Published:** December 16, 2013

   dx.doi.org/10.1021/bi401061e | *Biochemistry* 2014, 53, 115−126

central factors in the onset and progression of CVDs due to hypoxic exposure. It has also been shown that impaired NO availability plays an important role in the pathogenesis of hypoxia-induced vascular diseases.[16]

von Willebrand factor (vWF), an adhesive multimeric glycoprotein produced by endothelial cells, has an important function in primary hemostasis and also serves as a carrier protein of factor VIII.[17] It has also been established as a prognostic marker for different pathological conditions such as CPD, hypertension, and diabetes mellitus, for which ED is one of the prominent feature.[18,19] Previous studies have proven that the levels of plasma vWF increase in hypoxia-exposed animals because of ED.[20,21] A Framingham Offspring study by Frankel et al. showed that higher levels of vWF were associated with an increased risk of CVDs in people with type 2 diabetes mellitus or IR which was also associated with worse endothelial function and hemostatic imbalance.[18] These observations suggest that vWF might act as an inhibitor of insulin and antagonize insulin action. Therefore, we hypothesized that vWF inhibits insulin action by binding to NOS which simultaneously impairs insulin-induced NO production.

This study was designed with the following objectives: (1) to test whether vWF inhibits insulin-induced NO production and glucose metabolism during hypoxic exposure by using a glucose tolerance test (GTT), an insulin tolerance test (ITT), and D-[U-$^{14}$C]glucose uptake; (2) to test whether vWF binds directly to eNOS in RBCs or in a cell-free system; (3) to assess the binding affinity of vWF protein with eNOS in a cell-free system by surface plasma resonance spectroscopy (SPR); and (4) to analyze the binding kinetics of vWF with eNOS in RBCs.

We showed that vWF inhibits insulin-induced NO production in a dose-dependent manner, which subsequently impaired glucose metabolism. We also showed the existence of a novel direct protein−protein interaction between vWF and eNOS by using far-Western blotting, co-immunoprecipitation (CoIP), and the BIAcore technologies. The binding of vWF to eNOS inhibited insulin-induced NO production which led to IR *in vivo*.

## MATERIALS AND METHODS

**Ethical Clearance.** Protocols used in these studies were approved by the Internal Review Board, Defence Institute of Physiology and Allied Sciences. Studies were conducted in accordance with the Helsinki declaration of 1964. All volunteers who participated in the study were asked to sign an informed consent form before being included in the study. Adult Swiss albino mice weighing 25−30 g were used in this study. The mice were housed in the experimental animal facility of the institute and were fed a standard diet with deionized water on an *ad libitum* basis. All animal study protocols were approved by the institutional ethical committee of the Defence Institute of Physiology and Allied Sciences and the Ministry of Environment and Forest, Government of India.

**Blood Collection.** Blood was collected by venipuncture from volunteers using a 22 gauge siliconized needle. The blood was anticoagulated by adding 1 volume of 130 mM sodium citrate to 9 volumes of blood in plastic tubes and mixing by gentle inversion.

**Chemicals.** Human vWF (h-vWF; catalog no. ab88555) and rabbit polyclonal anti-eNOS antibody (catalog no. ab66127) were purchased from Abcam (Cambridge, MA). ECV-304 cell lysate (catalog no. SC-2269), goat polyclonal anti-vWF antibody (catalog no. SC8068), and protein A/G PLUS-agarose for immunoblotting and CoIP were from Santa Cruz Biotechnology Inc. (Santa Cruz, CA). Rabbit polyclonal anti-vWF antibody (catalog no. F3520) for immunoneutralization, phloretin, and L-arginine were purchased from Sigma-Aldrich (St. Louis, MO). D-[U-$^{14}$C]Glucose was from the Board of Radiation and Isotope Technology (Mumbai, India). eNOS protein (human origin), a kind gift from A. K. Sinha, was used as a positive control.[13] Mouse eNOS (catalog no. MBS954270) was purchased from MyBioSource, Inc. (San Diego, CA). Polyvinylidene difluoride (PVDF) membranes (ImmunoBlot PVDF) were purchased from Bio-Rad (Hercules, CA). Monocomponent human insulin (Human Mixtured) was procured from Torrent Pharmaceuticals Ltd. (Ahmedabad, India). Nitroglycerine (NG) patches were obtained from Novartis (Novartis TTS; Novartis India Ltd., Worli, Mumbai, India).

**Animal Treatment and Induction of Hypoxia.** h-vWF (100 $\mu$g/kg of body weight), rabbit anti-vWF neutralizing antibody [6.5 mg/kg of body weight; catalog no. F3520 (Sigma-Aldrich)] or rabbit nonimmune IgG (control) was delivered through tail vein injection 2 h prior to the GTT or ITT or homeostasis model of assessment insulin resistance (HOMA-IR) or hypoxic exposure (6−24 h) at the indicated times. NG patches (25 mg each) were applied to the dorsocervical area of the body which has been shaved normally on the same day of the experiment, and remained there throughout the experiments for the indicated times. Blood was withdrawn from retro-orbital veins through heparinized capillaries for HOMA-IR assays at the indicated times. Animals were subjected to hypoxia in a specially fabricated animal decompression chamber equivalent to the prevailing atmospheric conditions at an altitude of 7628 m (282 mmHg) having an $O_2$ content of ∼8.5% as described previously.[22] The temperature and humidity were maintained at 25 ± 2 °C and 60 ± 5%, respectively. Control animals were not placed in the decompression chamber but were otherwise treated in the same manner.

**NO Assay.** The synthesis of NO was assessed by using the conversion rate of oxyhemoglobin to methemoglobin through NO using a scanning spectrophotometer (Lambda 35, Perkin-Elmer, Norwalk, CT) as described by Jia et al.[23] Briefly, hypoxia-exposed plasmas were added to a reaction mixture containing Krebs buffer (pH 7.4) with 15 mM oxyhemoglobin, 10 mM L-arginine, and 240 nM insulin in a total volume of 2.5 mL for 45 min at 37 °C while the mixture was constantly stirred. The NO content was quantitated by recording the spectral changes in the reaction mixture due to the conversion of oxyhemoglobin to methemoglobin, i.e., a decrease in the absorbance at 575 and 630 nm maxima on a standard curve constructed by using pure commercial (>99% pure) NO in 0.9% NaCl under identical conditions. The amount of NO in the reaction mixture was confirmed by using an independent chemiluminescence technique.[24] Briefly, in the NO chemiluminescence analyzer, the 1 mM $NO_2^-$ standard was serially diluted (i.e., $10^{-9}$ to $10^{-3}$ mM) and added with 3 mL (1 M) of potassium iodide along with 3 mL (1 M) of HCl to the purge vessel which was then bubbled with helium for 5 min. The electrochemical signal generated by the product of each $NO_2^-$ standard was recorded and a standard curve was generated as a logarithmic function of nitrite dose (moles) versus chemiluminescence (millivolts). For the inhibition study, different concentrations of h-vWF or hypoxic plasma (100 $\mu$L/reaction) or saline (control) were incubated in this reaction mixture for 1 h before insulin was added.

**Enzyme-Linked Immunosorbent Assay.** An enzyme-linked immunosorbant assay was performed as described previously.[25] Briefly, 50 $\mu$g of plasma was incubated with an

equal volume of coating buffer [0.5 M carbonate buffer (pH 9.6)] in an assay plate overnight at 4 °C. Nonspecific binding was blocked by 5% bovine serum albumin in the same buffer. The samples were then washed with PBS containing 0.05% Tween 20 and incubated for 2 h with diluted rabbit anti-vWF primary antibody in blocking buffer (1:500). The samples were next washed and incubated with diluted goat anti-rabbit IgG-alkaline phosphatase (1:2000) in the same buffer for 2 h. After being washed, the samples were incubated with *p*-nitrophenyl phosphate (1 mg/mL) in carbonate buffer containing 10 mM $MgCl_2$. The development of color was assessed at 450 nm. The reaction was stopped by adding 50 μL of 1 M NaOH. The amount of vWF present in the sample was determined by constructing a standard curve using different amounts of h-vWF (purchased from abcam, catalog no. ab88555).

**Erythrocyte Membrane Preparation.** The erythrocyte membrane was prepared from human RBCs as described by Mihow et al.[26] Briefly, citrated blood was centrifuged at 4000*g* for 5 min at room temperature and pack cells were collected. Then, 500 μL of the pack cells was hemolyzed in 2 mL of ice-cold lysis buffer containing 10 mM Tris-HCl, 1 mM ethylenediaminetetraacetate, 10 μg/mL pepstatin A, 10 mM sodium pyrophosphate, and 10 mM NaF (pH 7.4). Membranes were pelleted at 47000*g* for 20 min at CR (Beckman Coulter Optima L 100K Ultracentrifuge, rotor SW 41 Ti). Next, the membranes were solubilized in lysis buffer containing 0.5% sodium deoxycholate and 1% Triton X-100. The protein concentrations of the samples were determined with the BCA protein assay (Pierce, Rockford, IL) using BSA as a standard.

**CoIP and Western Blotting.** CoIP of vWF and eNOS and their detection by Western blotting were conducted as described previously.[27] Briefly, RBC membranes were lysed in RIPA buffer [50 mM Tris-HCl (pH 7.4), 1% Nonidet P-40, 0.25% sodium deoxycholate, 150 mM NaCl, 1 mM ethylenediaminetetraacetate (EDTA), 1 mM NaF, 10 g/mL aprotinin, 10 g/mL leupeptin, and 1 mM phenylmethanesulfonyl fluoride]. Equal amounts of proteins were incubated with 0.5 μg of h-vWF protein for 4 h in a shaker at 4 °C followed by overnight incubation with 10 μL of rabbit polyclonal anti-eNOS antibody (1:1000 dilution). After being incubated with 25 μL of protein A/G PLUS-agarose beads at 4 °C for 2 h, the beads were washed thrice with phosphate-buffered saline and then boiled in sodium dodecyl sulfate−polyacrylamide gel electrophoresis (SDS−PAGE) sample buffer (1:1) for 5 min to elute proteins for subsequent electrophoresis. Western blotting was conducted as follows. The eluted proteins were resolved by 10% SDS−PAGE, transferred to a PVDF membrane, and subjected to immunoblotting using a goat polyclonal anti-vWF primary antibody (1:500). After incubation with a horseradish peroxidase-linked anti-goat secondary antibody, proteins were visualized by using an enhanced chemiluminescence detection system (Thermo Scientific, Rockford, IL).

**SDS−Agarose Electrophoresis.** For the analysis of vWF multimers, discontinuous thin-layer agarose electrophoresis was performed as described by Furlan et al.[28] using 1% agarose for high-resolution gels. Proteins were transferred to a PVDF membrane and subjected to immunoblotting using a goat polyclonal anti-vWF primary antibody and visualized with an enhanced chemiluminescence detection system as described above.

**Far-Western Blotting.** Far-Western blotting of vWF and eNOS was conducted as reported previously.[27] Briefly, 45−50 μg of protein from RBC lysates and 2 μg of purified eNOS proteins were boiled for 5 min in Laemmli sample buffer (1:1), resolved via 8% SDS−PAGE and transferred to PVDF membranes. After being incubated for 1 h with 1% casein (dissolved in Tris-buffered saline and 0.1% Tween), membranes were incubated with 2 μg of vWF protein for 3 h at 4 °C. The membranes were then washed with Tris-buffered saline and 0.1% Tween and incubated with an anti-vWF antibody (1:500) overnight at 4 °C. The membranes were washed again and incubated with the horseradish peroxidase-linked anti-goat IgG secondary antibody (1:2000) (Santa Cruz Biotechnology) for 1 h at room temperature. Finally, the resulting protein bands were detected with the ECL plus Western Blotting Detection System (Thermo Scientific).

**SPR Methodology.** The binding properties of vWF with eNOS protein were investigated via SPR. The BIAcore-2000 apparatus (Pharmacia Biosensor AB, Uppsala, Sweden), a biosensor-based system for real-time specific interaction analysis was used. The interaction of two biological molecules can be monitored directly by SPR. The phenomenon of SPR was studied by Otto[29] and Kretschmann and Raether[30] and used as a chemical detection method by Nylander.[31]

Sensor chip CM5 and the amine coupling kit containing *N*-hydroxysuccinimide, *N*-ethyl-*N*′-3-[(dimethylamino)propyl]-carbodiimide, and ethanolamine hydrochloride (Pharmacia Biosensor AB, Uppsala, Sweden) were used. The running buffer consisted of 10 mM HBS-EP (pH 7.4) containing 0.005% surfactant P20. Sensor chip CM5 is a disposable sensor chip. Its surface is covered with a thin gold layer coated with carboxymethyl dextran residues for covalent protein immobilization. The CM5 chip was purchased from Pharmacia Biosensor AB. The coated CM5 chip was used for protein immobilization. Immobilization of human eNOS or mouse eNOS protein was performed at a flow rate of 10 μL/min at 25 °C using the amine coupling kit. The dextran on the chip was equilibrated with running buffer and carboxymethylated and matrix-activated with an *N*-ethyl-*N*′-3-[(dimethylamino)propyl]carbodiimide/*N*-hydroxysuccinimide mixture. Then, 210 μL of eNOS protein (0.2 μg/μL) in 10 mM sodium acetate (pH 5.0) was injected and unreacted groups were blocked by injection of ethanolamine. Three different concentrations of ligand (h-vWF), i.e., 9.837, 19.675, and 29.513 nM were prepared in 10 mM HBS-EP buffer (pH 7.4). These samples were then injected separately in two different flow cells, i.e., one with immobilized eNOS protein and the other without ligand as a reference to remove nonspecific binding to the surface of the chip in different cycles at a flow rate of 10 μL/min at 25 °C. Dissociation of the ligand was performed by using 10 mM HBS-EP buffer (pH 7.4). Rate constants $K_A$ and $K_D$ were obtained by fitting the primary sensorgram data using BIA evaluation version 3.0. Regeneration of the ligand bound to the surface of the protein was achieved by using 1 mM NaOH. Kinetic parameters were obtained using BIA evaluation version 3.0. The association ($K_{on}$) and dissociation ($K_{off}$) rate constants for ligands binding to eNOS were calculated and the equilibrium ($K_D$) value was determined by using the mass action relation $K_D = K_{off}/K_{on}$.

**Kinetics and Inhibition Studies of the Protein by Spectrophotometry.** For the inhibition study, h-vWF was incubated in a reaction mixture containing 10 μM L-arginine (substrate) in Krebs buffer (pH 7.4) with 15 mM oxyhemoglobin for 1 h, prior to addition of 240 nM insulin. The change in absorbance was monitored at 575 and 630 nm and the percentage of inhibition was calculated. An experimental control was always included, i.e., a sample without h-vWF protein.

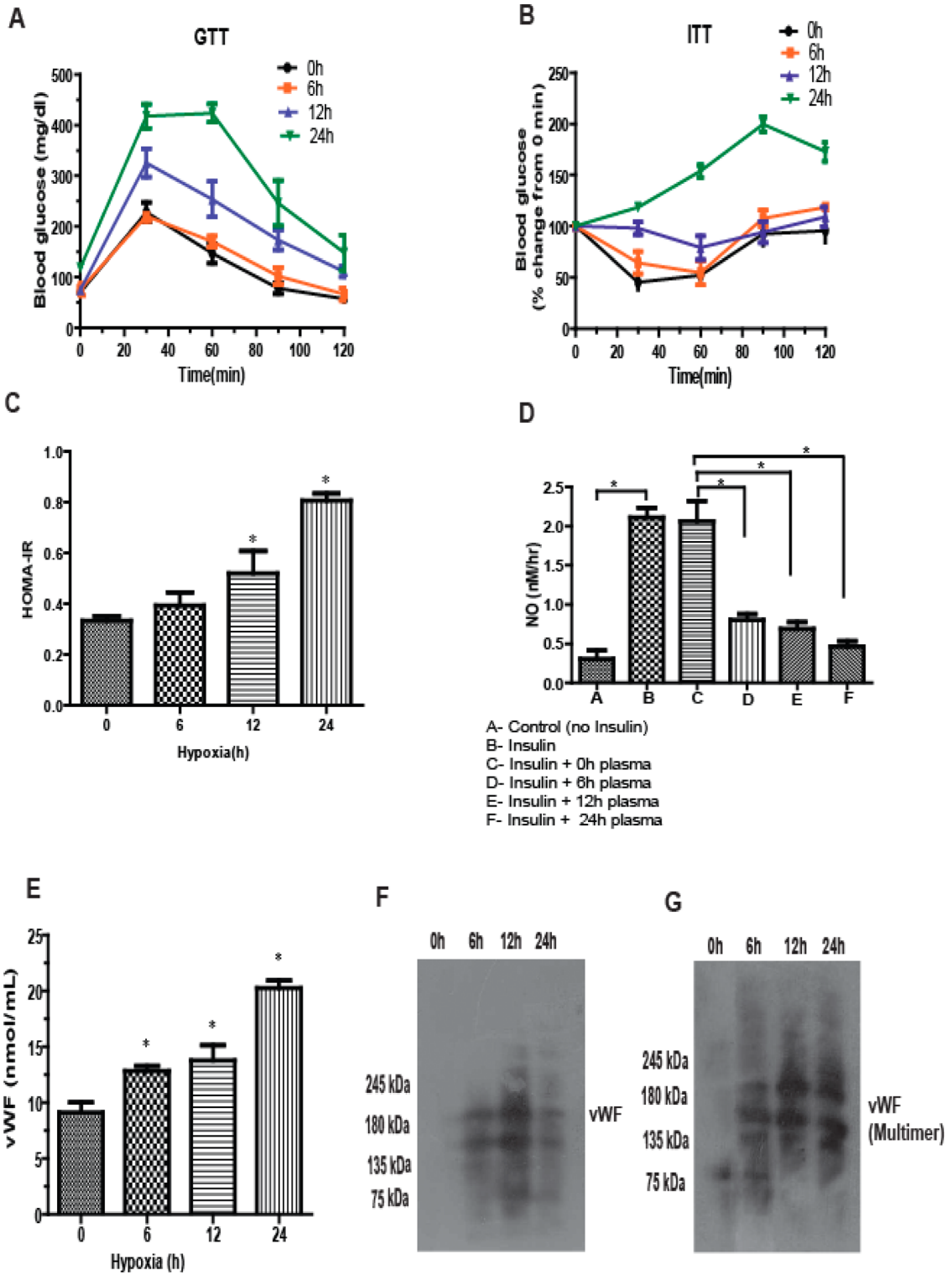


**Figure 1.** Time course study of the effect of hypoxia on glucose metabolism and ED. Animals were exposed to hypoxia as described in Materials and Methods for 0 (unexposed), 6, 12, and 24 h. The GTT, ITT, and HOMA-IR were conducted for IR study, and SDS immunoblotting, an ELISA of vWF, and the NO assay were preformed for ED. (A) A glucose tolerance test was performed after a 16 h fast ($n = 4$ per group). (B) An insulin tolerance test (0.75 unit/kg of insulin) was performed in random-fed mice for different periods of hypoxia ($n = 4$ per group). (C) The insulin resistance test was performed by HOMA-IR score in hypoxia-exposed mice ($n = 4$ per group). (D) Insulin-induced NO production was inhibited by addition of plasma of different AH-exposed animals. (E) Quantitation of vWF total antigen by an ELISA in plasma ($n = 4$ per group). (F) Immunoblotting of vWF at different time points. (G) Multimer analysis of vWF by SDS−agarose gel electrophoresis followed by immunobotting for the indicated time points. Results are from a representative experiment from three independent experiments. Data are means ± SEM of three separate experiments. The results show a significant (*$p < 0.05$) difference between different time points using one-way ANOVA.


dx.doi.org/10.1021/bi401061e | *Biochemistry* 2014, 53, 115−126

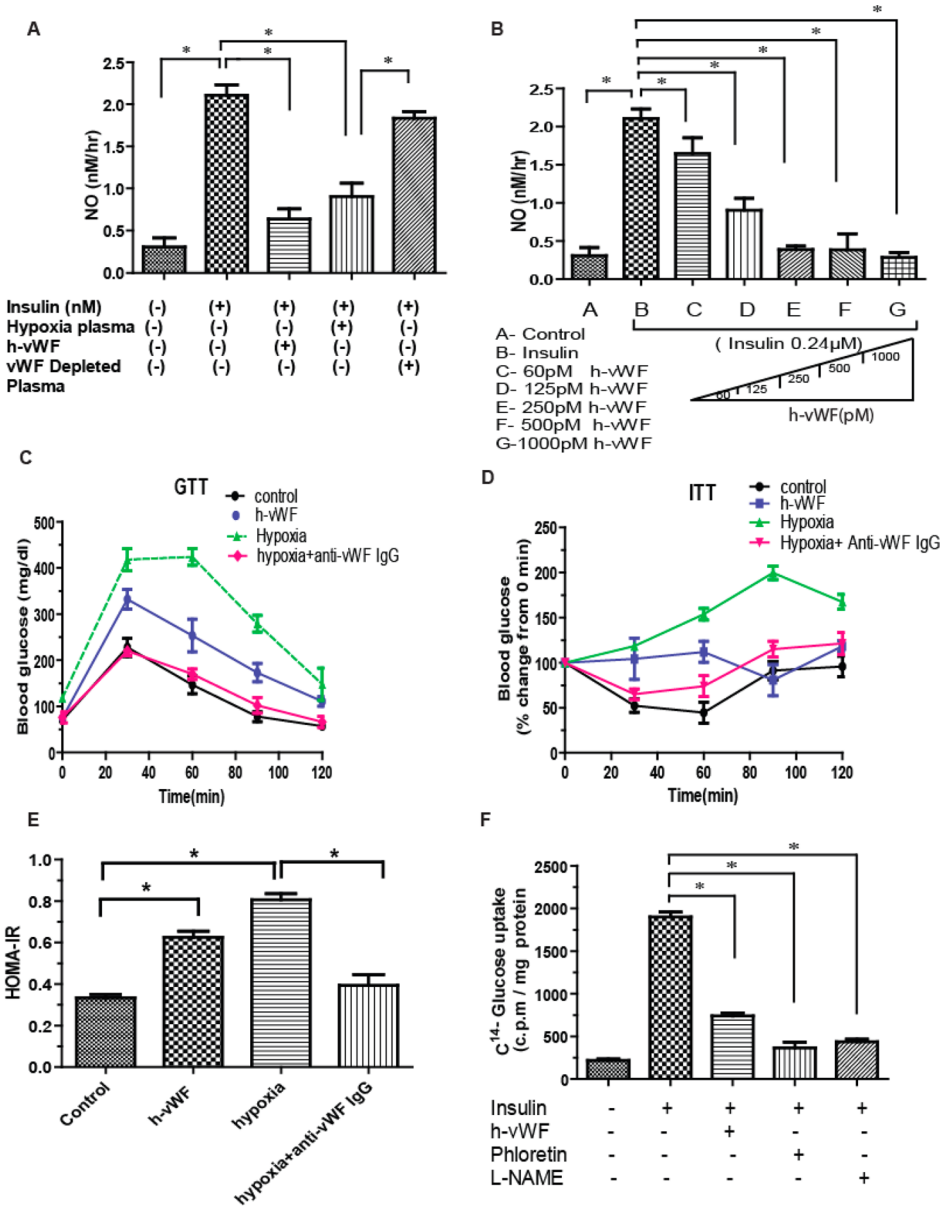


**Figure 2.** Central role of vWF in inhibition of insulin-induced NO synthesis and glucose hemostasis. (A) Insulin-induced NO production was inhibited by addition of plasma of hypoxia-exposed (24 h) animals and h-vWF, but addition of vWF immunodepleted plasma in the reaction mixture restored the insulin-induced NO production. (B) Addition of different doses of h-vWF to the reaction mixture inhibits insulin-induced NO production dose-dependently. (C–E) GTT, ITT, and HOMA-IR in hypoxia/h-vWF as well as anti-vWF neutralizing antibody (2 h before) infused in mice ($n$ = 4 per group). (F) The uptake of D-[U-$^{14}$C]glucose by insulin was measured in RBCs pretreated with either h-vWF, phloretin, or L-NAME. Data are means ± SEM of three separate experiments. The results show a significant (*$p < 0.05$) difference between different time points using one-way ANOVA.

For the kinetic assay, the experiment described above was conducted with five different concentrations of h-vWF (60–1000 pM). For each concentration of h-vWF, the experiment was repeated with three different concentrations (0.24–1.2 $\mu$M) of an activator, i.e., insulin. The enzyme and substrate concentrations were constant throughout the assay. The enzyme inhibitor constant ($K_i$) and half-maximal inhibitory concentration ($IC_{50}$) were calculated graphically using the Michaelis–Menten equation in GraphPad Prism version 5.0. A graph of activity versus concentration of insulin was plotted.

**D-[U-$^{14}$C]Glucose Uptake.** RBCs were incubated with insulin in the absence or presence of h-vWF for 4 h followed by stimulation with insulin (240 nM) for 30 min. D-[U-$^{14}$C]-Glucose (0.4 nM/mL) was added to each incubation mixture 5 min before termination of the experiment. Cells were washed three times with ice-cold Krebs-Ringer Buffer in the presence of 0.3 mM phloretin and then lysed with hypotonic lysis buffer [1 M $NaH_2PO_4$/$NaHPO_4$ (pH 8.0)]. D-[U-$^{14}$C]Glucose uptake was measured in a liquid scintillation counter (Tri-Carb 2800TR LSA, Perkin-Elmer).

**GTTs.** Mice were fasted for 16 h before the GTT was performed. The GTT was conducted as follows. After blood had been collected from the tail vein (0 h), mice received glucose (2 g/kg of body weight) via intraperitoneal (ip) injection, and blood glucose levels were measured at 0, 30, 60, 90, and 120 min by using the Accu-Chek glucometer (Roche).

**ITTs.** The insulin tolerance test was performed on randomly fed animals between 2:00 and 5:00 p.m. Animals were injected


dx.doi.org/10.1021/bi401061e | *Biochemistry* 2014, 53, 115–126

(ip) with monocomponent human insulin (0.75 unit/kg of body weight). Blood glucose levels were determined immediately before and 30, 60, 90, and 120 min after injection. Results were expressed as the percentage change compared to the initial blood glucose concentration.

**IR.** IR was assessed by HOMA-IR as described by Mathew et al.[32] The plasma insulin level was estimated by using an electrochemiluminescence assay (Roche Diagnostics, Manheim, Germany).

**CT.** The blood clotting time was measured as described by Lemini et al.[33] Briefly, the tails of the untreated WT mice and WT mice treated with the anti-vWF antibody (6.5 mg/kg of body weight) were warmed for 1 min in water at 40 °C. The tails were dried and cut at the tips with a sterilized razor blade. A 25 $\mu$L sample of the capillary blood was collected into a microhematocrit glass capillary. The stopwatch was started when the blood first made contact with the glass capillary tube. The blood was left to flow by gravity between two marks of the tube, 45 mm apart, by tilting the capillary tube alternately +60° and −60° angles with respect to the horizontal plane until blood ceased to flow (reaction end point).

**BT.** The BT was performed as described by Dejana et al.[34] Briefly, untreated WT mice and WT mice treated with the anti-vWF antibody (6.5 mg/kg of body weight) were maintained in a restrainer and a distal 2 mm segment of the tail was severed with a razor blade. The tail was immediately immersed in 0.9% isotonic saline at 37 °C with the tip of the tail 5 cm below the body. The BT was defined as the time required for the stream of blood to cease.

**Statistical Analysis.** All experiments were repeated at least three times. Data are expressed as means ± the standard error of the mean. The statistical analysis of differences between experimental groups was performed by one-way analysis of variance (ANOVA). A $p$ value of $<0.05$ was considered statistically significant. Further statistical analysis was performed by Bonferroni's multiple-comparison tests.

## RESULTS

**Effect of Hypoxia on Glucose Homeostasis and ED.** Experiments were conducted to determine the time-dependent effect of hypoxia on glucose metabolism and ED. It was found that animals exposed to hypoxia showed time-dependent increases in GTT, ITT, and HOMA-IR values in comparison to those of control animals (Figure 1A−C). We further showed the time-dependent inhibition of NO production (Figure 1D) and time-dependent upregulation of multimeric forms of vWF in the plasma of hypoxia-exposed animals in comparison to those of control animals (Figure 1E−G). These results suggest that hypoxia induces ED as well as glucose intolerance in a time-dependent manner.

**Hypoxia-Induced vWF Inhibits NO Synthesis and IR.** The results described above as well as those of an earlier study showed that exposure to hypoxia reduces NO production *in vivo*.[35] However, the mechanism of inhibition of NO synthesis *in vivo* is not clearly understood. Studies were conducted to test whether vWF has any role in the inhibition of insulin-induced NO production and induction of IR. It was found that addition of plasma of hypoxia-exposed animals and h-vWF to the reaction mixture inhibits insulin-induced NO production (Figure 2A). To establish the role of vWF, we used vWF-immunodepleted plasma in the same reaction mixture. The results showed that immunodepletion failed to inhibit insulin-induced NO synthesis (Figure 2A). To revalidate the inhibitory role of vWF in insulin-induced NO synthesis, we determined the NO synthesis rate in the presence of different concentrations of h-vWF (60−1000 pM) in the reaction mixture. The results showed that preincubation of the reaction mixture with h-vWF significantly inhibited insulin-induced NO synthesis in a dose-dependent manner (Figure 2B). Optimal inhibition was noted at 125 pM vWF. Considering this result, we used 125 pM vWF in the subsequent experiments. These results suggest that vWF acts as an inhibitor of insulin-induced NO synthesis.

It has been established that insulin-induced glucose uptake is mediated through NO, a second-messenger molecule of insulin.[15] The involvement of vWF in IR has been shown previously.[18] To evaluate the possible role of vWF on IR due to inhibition of NOS, we performed GTT, ITT, HOMA-IR, and glucose uptake studies on either hypoxia-exposed or h-vWF-treated animals. Animals exposed to hypoxia or h-vWF were prone to IR, as evident by increased GTT (Figure 2C), ITT (Figure 2D), and HOMA-IR scores (Figure 2E) and decreased levels of D-[U-$^{14}$C]glucose uptake (Figure 2F). On the other hand, pretreatment with a vWF immunoneutralizing antibody 2 h prior to hypoxia exposure blocked the inhibitory effect of vWF on glucose metabolism (Figure 2C−E). Interestingly, antibody-mediated vWF immunoneutralization did not alter the BT or CT (Tables 1A and 1B of the Supporting Information). These results suggest that vWF inhibits insulin-induced NO production and IR.

**NO in Hypoxia-Induced IR.** Experiments were conducted to reconfirm the role of NO in hypoxia-induced IR. We conducted a series of experiments in which we applied NO mimetic nitroglycerine (NG) patches transdermally to mice. Our results showed that transdermal application of NG patches averts hypoxia-induced IR [i.e., GTT (Figure 3A), ITT (Figure 3B) and HOMA-IR (Figure 3C)], whereas treatment with the NO inhibitor L-NAME also causes IR (Figure 3A−C). This observation suggests that hypoxia-induced IR is mediated through inhibition of insulin-induced NO production.

**Larger Doses of Insulin Prevent vWF-Mediated Inhibition of Insulin-Induced NO Synthesis.** Experiments were conducted to analyze whether the inhibition of insulin-induced NO synthesis by vWF is prevented by larger doses of insulin. We found that larger doses of insulin (0−1200 nM) in the reaction mixture prevented the inhibitory effect of vWF in a dose-dependent manner (Figure 4). These results suggest that binding of insulin to eNOS is competitively inhibited by vWF and consequently inhibits NO production. In other words, it suggests that vWF and insulin compete for the same binding site of eNOS.

**Binding of vWF to eNOS Detected with Far-Western Blotting and CoIP.** From the results mentioned above, we can infer that vWF binds indirectly to eNOS and inhibits NO production. To obtain direct evidence of the binding, we first performed far-Western blotting with RBC membrane lysates expressing native eNOS, serving as the target prey probed with h-vWF protein as bait protein, as detailed in Materials and Methods.

Purified human eNOS protein was used as a positive control, whereas eNOS-lacking ECV-304 cell lysate served as a negative control.[36,37] Binding of the prey protein to the bait proteins was detected with a specific anti-vWF antibody. In the lanes containing the RBC membrane lysate and eNOS, h-vWF bound to a 130 kDa protein, which matched the size of this molecule (Figure 5A). No band was detected in the lane containing the ECV-304 cell lysate (negative control). Then, the

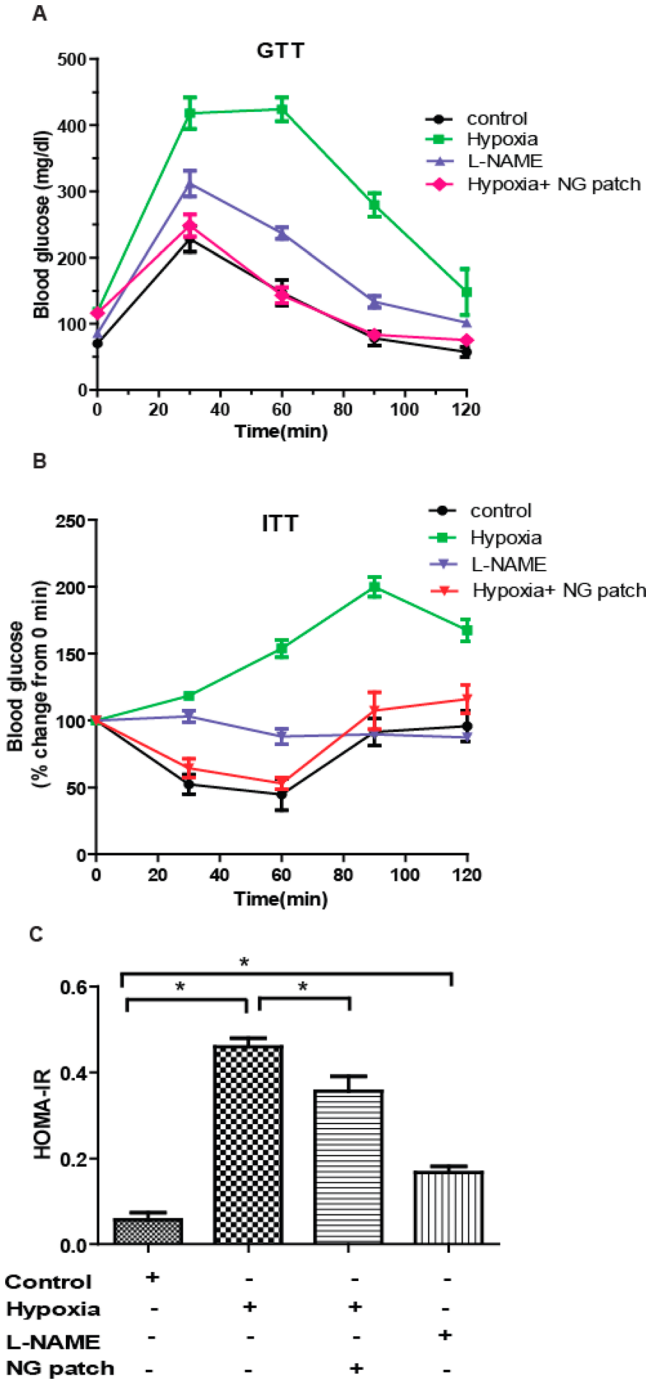


**Figure 3.** In hypoxia, vWF induces IR in a NO-dependent manner. (A) GTT, (B) ITT, and (C) HOMA-IR in control, hypoxia-exposed, L-NAME-treated, and nitroglycerine (NG) patch-treated mice. The application of the NG patch reverses the effects of hypoxia, but the L-NAME (70 mg/kg of body weight) treatment significantly increases GTT, ITT, and HOMA-IR scores. Data are means ± SEM of three separate experiments. The results show a significant (*$p$ < 0.05) difference between different time points using one-way ANOVA.

membrane was stripped and reprobed with a rabbit monoclonal eNOS antibody. A 130 kDa band was detected in both lanes, i.e., those containing the RBC membrane lysate and eNOS (Figure 5B). No band was detected in the lane containing the ECV-304 cell lysate. Taken together, these results revealed the specific binding of vWF to eNOS contained in RBC cells as well as in the cell-free system.

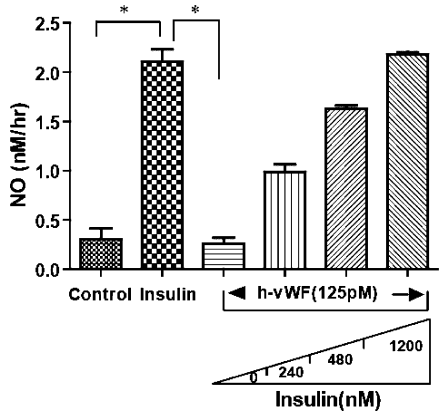


**Figure 4.** vWF-mediated inhibition of NO production reversed by larger doses of insulin. Addition of larger doses of insulin dose-dependently (0−1200 nM) to the reaction mixture eliminates the inhibitory effect of vWF. Data are means ± SEM of triplicate reactions from three separate experiments. The results showed a significant (*$p$ < 0.05) difference in comparison to the control using one-way ANOVA.

To revalidate the far-Western blotting result, we performed CoIP experiments. eNOS was immunoprecipitated by vWF and the subsequent vWF antibody from RBC membrane lysates (experimental), purified eNOS (positive control), and ECV-304 cell lysate (negative control) detailed in Materials and Methods. The immune complexes were resolved by SDS−PAGE and immunoblotted for eNOS protein. Figure 5C again shows clearly identical bands of 130 kDa in the lanes containing RBC membrane lysate and purified eNOS, but no band was seen in ECV-304 cell lysate, proving that eNOS co-immunoprecipitated with vWF.

In another experiment, we immunoprecipitated vWF from hypoxia-exposed animal plasma (experimental) and h-vWF (positive control) by purified eNOS protein and immunoblotted the samples for vWF. The results showed that vWF immunoprecipitated with eNOS; i.e., the 180 kDa band of vWF was detected in hypoxia-exposed plasma (experimental) and h-vWF (positive control) (Figure 5D). However, in the case of vWF, the same molecular mass band was noted (Figure 5D). These results further confirm the specific binding of vWF to eNOS in RBCs.

**Determination of $K_D$ by SPR.** Figure 6 shows the sensorgram for the binding of the analyte (h-vWF) at varying concentrations to immobilized human eNOS or mouse eNOS protein on the CM5 sensor chip. The change in the response units with varying ligand concentrations indicated the change in the bound mass on eNOS immobilized on the chip (sensor surface) over time. The binding of h-vWF to human eNOS was the strongest because of the faster "on" rate (association constant) ($K_A$ = 5.6 × $10^7$ M) as well as the slower "off" rate (dissociation constant) [$K_D$ = 1.79 × $10^{-8}$ M (Figure 6A)]. On the other hand, the binding of h-vWF to mouse eNOS was also same [$K_A$ of 5.62 × $10^7$ M and $K_D$ of 1.75 × $10^{-8}$ M (Figure 6B)]. These data suggest that h-vWF binds to human or mouse eNOS with affinity.

**Kinetic Analysis of NO Production.** The kinetic mechanisms of eNOS (enzyme), insulin (activator), and vWF (inhibitor) were assessed by varying the concentrations of insulin and h-vWF. The competitive kinetic constant of vWF was calculated using GraphPad Prism version 5.0. A linearized analysis of the data (Michaelis−Menten equation) revealed a competitive mode of inhibition (Figure 7A). By using the


dx.doi.org/10.1021/bi401061e | *Biochemistry* 2014, 53, 115−126

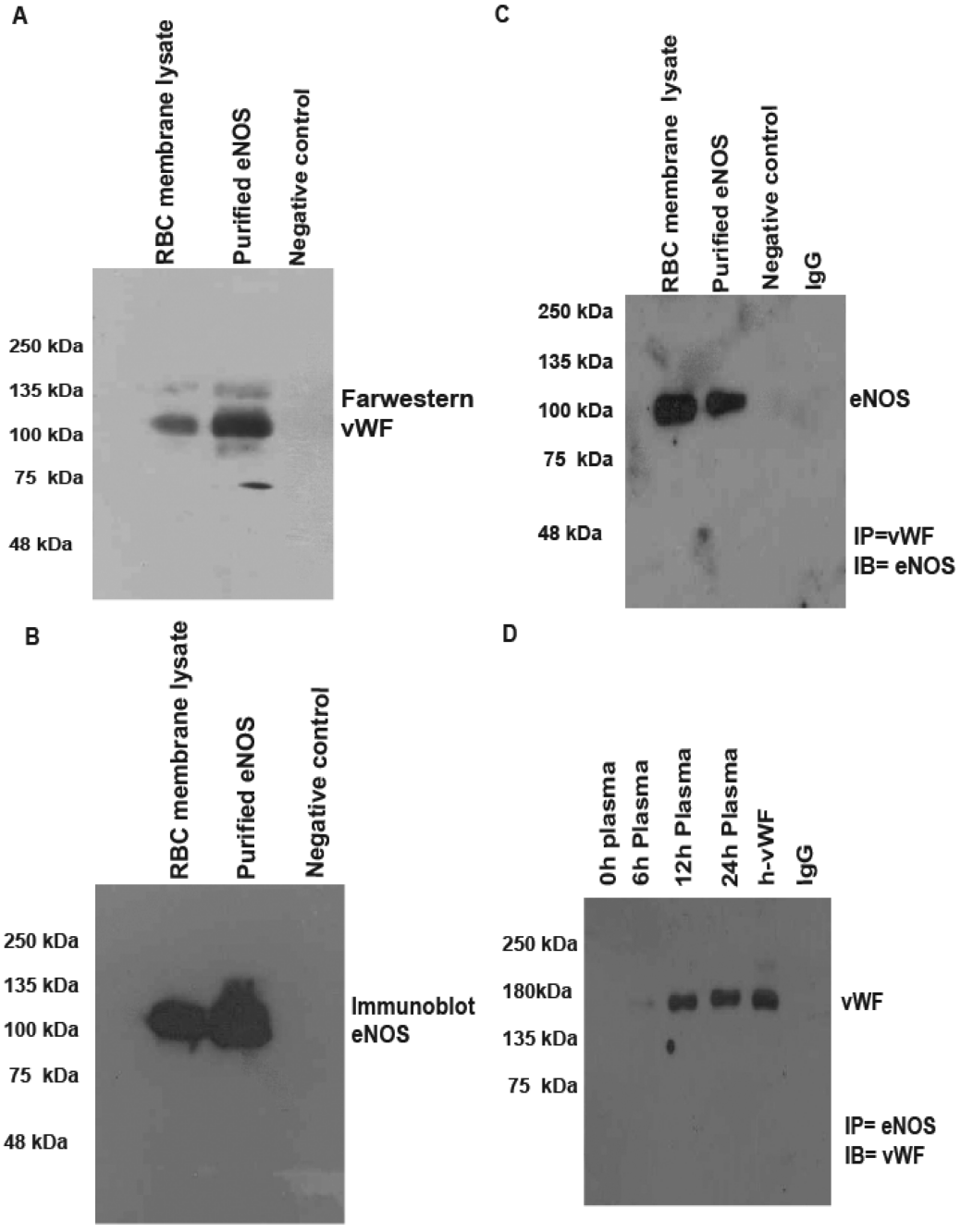


**Figure 5.** Far-Western blot analysis and CoIP of binding of NOS to vWF. (A) We used purified human eNOS (positive cell-free control), RBC lysate protein (experimental sample), and eNOS-negative ECV-304 cell lysate protein (negative control). The immune-positive bands were detected using the anti-vWF antibody, revealing a 130 kDa band representing the eNOS in both RBC membrane lysate and purified eNOS. (B) The same membrane was striped and reprobed with the anti-eNOS antibody, revealing that of a 130 kDa band. (C) RBC membrane lysate (experimental sample), purified eNOS (positive cell-free control) and ECV-304 cell lysate (negative control) were incubated with h-vWF protein to pull down the eNOS using the anti-vWF antibody. Western blot analysis was performed with the anti-NOS antibody. The detected signals corresponded to the eNOS protein (130 kDa) in both RBC membrane lysate and purified eNOS. No band was observed in ECV-304 cell lyaste (negative control). IgG served as the negative control. (D) h-vWF (positive cell-free control) and plasma exposed to hypoxia for different periods of time (experimental samples) were incubated with purified eNOS protein to pull down the vWF using the anti-eNOS antibody. Western blot analysis was performed with the anti-vWF antibody. The detected signals corresponded to the vWF protein (180−150 kDa) in both h-vWF and exposed samples. IgG served as the negative control. These experiments were reproduced thrice. IB, immunoblot; IP, immunoprecipitation. Results are from a representative experiment from three independent experiments.

double-reciprocal plot, the values of $1/K_m$ and $1/V_{max}$ were quantified; the former increased in the presence of vWF, while the later remained unchanged, proving the competitive mode of inhibition between the two substrates (Figure 7B). The $IC_{50}$ and $K_i$ values obtained for vWF were 18.31 pM (Figure 7C) and 250 pM (Figure 7D), respectively. The lower $K_i$ value suggests a higher efficacy of the inhibitor (vWF) for activator (insulin) inhibition. On the other hand, a higher $IC_{50}$ value denotes the higher potency of the inhibitor. The direct plots of reaction velocity versus substrate concentration demonstrated classical steady-state kinetic behavior. Best fits for experimental data were assessed by comparison of the standard errors of the mean;


dx.doi.org/10.1021/bi401061e | *Biochemistry* 2014, 53, 115−126

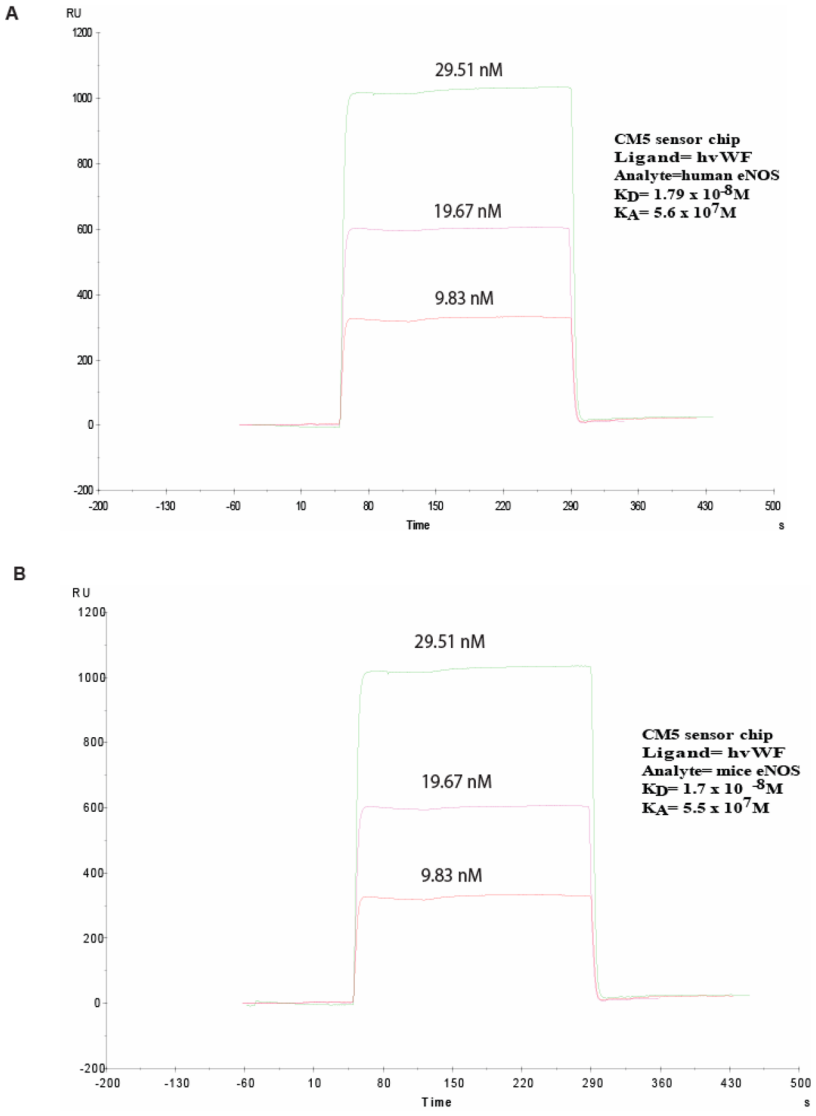


**Figure 6.** Surface plasma resonance analysis of binding of vWF to human eNOS or mouse eNOS. Sensorgram showing binding of different concentrations of vWF (9.85, 19.67, and 29.51 nM) immobilized with purified human eNOS or mouse eNOS protein over sensor chip CM5. There is no change in the binding affinity of human vWF with human eNOS or mouse eNOS (RU, response units). Experiments were performed at least three separate times, and typical results are shown.

nonlinear regression analysis *F* tests were employed for competitive inhibition fits.

## DISCUSSION

This study investigated the relationship between increased levels of vWF release and decreased levels of NO production and insulin sensitivity during hypoxia. Using biochemical as well as functional approaches, this study reveals for the first time that vWF is a novel ligand for eNOS. vWF antagonizes insulin action, impairs NO production, and elicits changes in glucose homeostasis with increases in results of the GTT, ITT, and HOMA-IR and a decrease in the rate of glucose uptake in an animal model of hypoxia. The binding of vWF to eNOS was demonstrated in RBC membranes and in a cell-free system (purified eNOS) by far-Western blotting and CoIP. This interaction was also confirmed by SPR in a cell-free system. We further demonstrated that the binding of vWF to eNOS impaired insulin-induced NO production and increased IR; however, larger doses of insulin reversed the inhibitory effect of vWF.

Recently, data from epidemiological cohort studies and clinical populations have determined that OSA may contribute to the development of IR.[2,38] It was also reported that exposure to acute hypoxia increased glucose intolerance in healthy men and women.[4,5] Lee et al. also showed that acute 1 day exposure to intermittent or continuous hypoxia resulted in impaired glucose tolerance, reduced insulin sensitivity, and an increased level of secretion of insulin from the pancreas.[39] In our study, we also reported time-dependent increases in results of the GTT, ITT, and HOMA-IR (exposure to hypoxia for up to 24 h), which supports previous findings. Peltonen and co-workers recently reported that acute exposure to hypoxia decreases insulin sensitivity through sympathetic activation.[40] Gamboa et al. also showed that either acute exposure or continuous hypoxia can induce IR.[41]Therefore, all previous studies and ours arrive at the same conclusion. However, the molecular mechanism of IR during hypoxia is still obscure. Previous studies proposed a relationship between CVDs, IR, and ED, where ED has been


dx.doi.org/10.1021/bi401061e | *Biochemistry* 2014, 53, 115−126

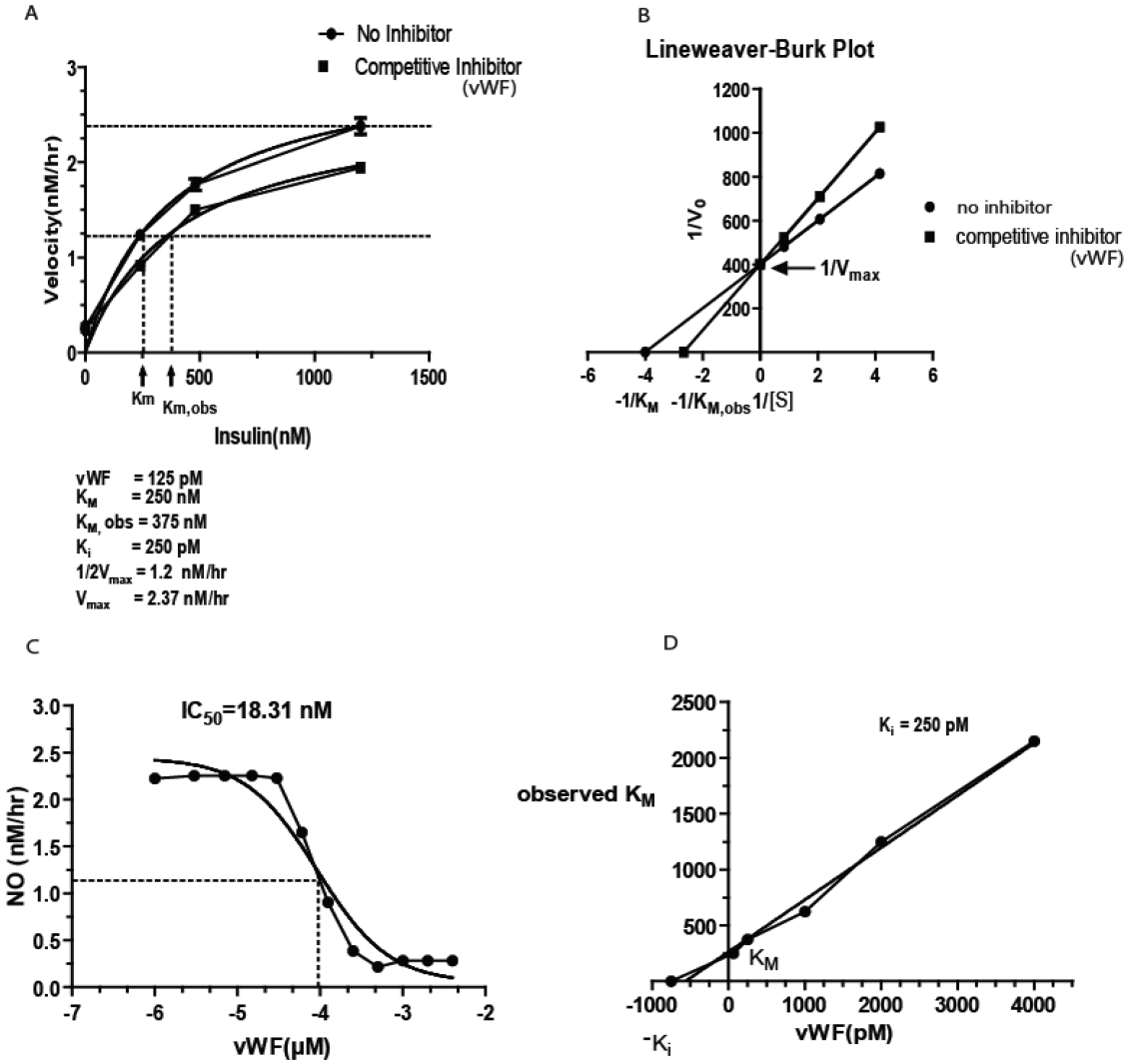


**Figure 7.** Enzyme kinetics of eNOS inhibition. (A) Enzyme kinetic analysis of eNOS inhibition by vWF using the Michaelis−Menten equation. (B) Lineweaver−Burk plots of reaction velocity vs substrate concentration for enzyme kinetics of eNOS in the absence and presence of vWF. The values of $IC_{50}$ (C) and $K_i$ (D) for vWF in displacing insulin binding were 18.31 nM and 250 pM, respectively. Results are from a representative experiment from three independent experiments. Experiments were performed at least three separate times, and mean values are shown. All the analysis was done by using GraphPad Prism version 5.0 (GraphPad Software, Inc., La Jolla, CA).

characterized by an increased rate of vWF release and a decreased level of NO production.[18,42] Impaired NO production, a phenotype of IR, has also been linked to OSA and CVDs.[43,44]

Diabetes mellitus and IR have also been associated with worse endothelial function and treatment with thiazolidinediones (insulin sensitizers) has been shown to improve ED.[43] Our results also demonstrated a time-dependent upregulation of multimeric forms of vWF in plasma and subsequent inhibition of NOS activity. We further demonstrated that vWF-immunodepleted hypoxic plasma failed to inhibit insulin-induced NO production and h-vWF also inhibited insulin-induced NO production in a dose-dependent manner. On the other hand, larger doses of insulin reversed the effects. In contrast, blockade of vWF by a neutralizing antibody attenuated hypoxia-induced IR, as demonstrated by the GTT, ITT, and HOMA-IR without altering the bleeding phenotype. This suggests that vWF might play a crucial role in hypoxia-induced IR through inhibition of NOS and established an inverse relationship between vWF and NO production during hypoxia. To reconfirm the role of NO in hypoxia-induced IR, we used NO-mimetic NG patches that were transdermally applied to mice and prevented hypoxia-induced IR. This finding also suggests that hypoxia-induced IR is mediated through inhibition of NO production. To further determine the biological relevance of hypoxia-induced upregulation of vWF and a decreased rate of glucose uptake through NO inhibition, we used h-vWF in our D-[U-$^{14}$C]glucose uptake assay. Preincubation with either h-vWF or L-NAME completely abrogated insulin-induced glucose uptake in RBCs. In this study, we further demonstrated that the continuous delivery of NO elicited by the application of a transdermal NG patch protected mice from IR. This result suggests that vWF inhibits glucose uptake by inhibiting NO synthesis through inhibition of NOS.

The biological significance of the antagonizing effect of vWF on NO production through direct interaction with NOS is profound. By using far-Western blotting, CoIP, and SPR, our study demonstrated for the first time the direct interaction between vWF and NOS. Our data suggest that vWF inhibits insulin-induced NO production by directly binding to eNOS. A previous study had also established that NOS is the receptor and


dx.doi.org/10.1021/bi401061e | *Biochemistry* 2014, 53, 115−126

NO is a second messenger for insulin action.[15] It was also reported that eNOS is a membrane-bound constitutive enzyme whose activation is directly related to the binding of insulin to its specific binding sites on the membrane surface.[15] Here, we performed SPR to determine the affinity of the interaction between vWF and NOS. The resulting sensorgram showed concentration-dependent binding of both molecules and the affinity of the binding was considerably high, as indicated by a $K_D$ of $1.79 \times 10^{-8}$ M. This finding was further validated by kinetic analyses of both molecules. The results showed a noticeably low inhibitory constant ($K_i$ = 250 pM), as well as $IC_{50}$ (18.31 pM), suggesting a higher affinity of binding to and greater efficacy of inhibition of eNOS by vWF. Under normal conditions, the physiological concentrations of insulin and vWF are 542 and 5.2 nM, respectively;[45] therefore, vWF never binds to eNOS because the affinity is lower than that for insulin ($K_d = 2.45 \times 10^{-9}$ M).[13] However, under several pathological conditions where the concentration of the ultralarge form of vWF is higher than normal,[46] insulin-induced NO production is inhibited by competitive binding of vWF to NOS.

It was also reported that NO has a role in glucose transport and metabolism in rat skeletal muscle through NOS activation.[47] Our results indicate that vWF acts as an inhibitor of NOS and impaired insulin action and NO production. Upon binding to its receptor (NOS), insulin stimulates NO production, which in turn activates the Glut-4 receptor, consequently leading to an increased rate of glucose uptake but a decreased level of platelet aggregation.[48,49] However, a putative predictive functional region of vWF is shown in Supplement 2 of the Supporting Information. However, details of the interaction between the two molecules remain to be explored and the importance of a specific domain and/or sequence of the respective protein still needs to be studied.

This study delineates the mechanism of inhibition of NO production by vWF during hypoxia, where ED is the predominant feature. It might also explain the mechanism of increased IR in patients with CVDs and diabetes mellitus. The data of this study may have important implications for glucose homeostasis at high altitude and the risk for metabolic diseases for patients with disorders characterized by hypoxia, sleep apnea, and chronic obstructive pulmonary disease.

## ■ ASSOCIATED CONTENT

### Supporting Information

Determination of clotting time (CT) (Table 1A), determination of bleeding time (BT) (Table 1B), and putative interaction of vWF (residues 2597−2791) with the insulin receptor (Supplement 2). This material is available free of charge via the Internet at http://pubs.acs.org.

## ■ AUTHOR INFORMATION


### Corresponding Author

*Department of Physiology, Defence Institute of Physiology and Allied Sciences, Lucknow Road, Timarpur, New Delhi 110054, India. Telephone: +91-11-23883214. Fax: +91-11-239-14790. E-mail: gausalk@gmail.com.



### Funding

This work is supported by grants from the Defence Institute of Physiology and Allied Sciences, Ministry of Defence, Government of India (TASK-158 and DIP-255), to G.A.K.


### Notes

The authors declare no competing financial interest.

## ■ ACKNOWLEDGMENTS


We sincerely thank Dr. Sudhanshu Vrati (National Institute of Immunology, New Delhi, India) for his assistance with the radioactive experiments.


## ■ ABBREVIATIONS

AH, acute hypoxia; IR, insulin resistance; ELISA, enzyme-linked immunosorbent assay; IANOS, insulin-activated nitric oxide synthase; GTT, glucose tolerance test; ITT, insulin tolerance test; BT, bleeding time; CT, clotting time; SPR, surface plasma resonance spectroscopy; CVD, cardiovascular disease; SDS, sodium dodecyl sulfate; PAGE, polyacrylamide gel electrophoresis; RIPA, radioimmunoprecipitation assay; ED, endothelial dysfunction; RBC, red blood cell; Ins, insulin; vWF, von Willebrand factor; L-Arg, L-arginine; EC, endothelial cell; SMC, smooth muscle cells; IB, immunoblot; CoIP, co-immunoprecipitation; RU, response units; NG, nitroglycerine; NO, nitric oxide; eNOS, endothelial nitric oxide synthase; SEM, standard error of the mean.

## ■ REFERENCES


(1) Oltmanns, K. M., Gehring, H., Rudolf, S., Schultes, B., Rook, S., Schweiger, U., Born, J., Fehm, H. L., and Peters, A. (2004) Hypoxia causes glucose intolerance in humans. *Am. J. Respir. Crit. Care Med. 169*, 1231−1237.

(2) Punjabi, N. M., Sorkin, J. D., Katzel, L. I., Goldberg, A. P., Schwartz, A. R., and Smith, P. L. (2002) Sleep-disordered breathing and insulin resistance in middle-aged and overweight men. *Am. J. Respir. Crit. Care Med. 165*, 677−682.

(3) Lanfranchi, P., and Somers, V. K. (2001) Obstructive sleep apnea and vascular disease. *Respir. Res. 2*, 315−319.

(4) Larsen, J. J., Hansen, J. M., Olsen, N. V., Galbo, H., and Dela, F. (1997) The effect of altitude hypoxia on glucose homeostasis in men. *J. Physiol. 504* (Part 1), 241−249.

(5) Braun, B., Rock, P. B., Zamudio, S., Wolfel, G. E., Mazzeo, R. S., Muza, S. R., Fulco, C. S., Moore, L. G., and Butterfield, G. E. (2001) Women at altitude: Short-term exposure to hypoxia and/or $\alpha_1$-adrenergic blockade reduces insulin sensitivity. *J. Appl. Physiol. 91*, 623−631.

(6) Kuboki, K., Jiang, Z. Y., Takahara, N., Ha, S. W., Igarashi, M., Yamauchi, T., Feener, E. P., Herbert, T. P., Rhodes, C. J., and King, G. L. (2000) Regulation of endothelial constitutive nitric oxide synthase gene expression in endothelial cells and in vivo: A specific vascular action of insulin. *Circulation 101*, 676−681.

(7) Montagnani, M., Chen, H., Barr, V. A., and Quon, M. J. (2001) Insulin-stimulated activation of eNOS is independent of $Ca^{2+}$ but requires phosphorylation by Akt at Ser(1179). *J. Biol. Chem. 276*, 30392−30398.

(8) Zeng, G., Nystrom, F. H., Ravichandran, L. V., Cong, L. N., Kirby, M., Mostowski, H., and Quon, M. J. (2000) Roles for insulin receptor, PI3-kinase, and Akt in insulin-signaling pathways related to production of nitric oxide in human vascular endothelial cells. *Circulation 101*, 1539−1545.

(9) Lurie, A. (2011) Endothelial dysfunction in adults with obstructive sleep apnea. *Adv. Cardiol. 46*, 139−170.

(10) Liebler, D. C. (2008) Protein damage by reactive electrophiles: Targets and consequences. *Chem. Res. Toxicol. 21*, 117−128.

(11) Lusis, A. J. (2000) Atherosclerosis. *Nature 407*, 233−241.

(12) Girish, G. V., Bhattacharya, G., and Sinha, A. K. (2006) The role of insulin dependent NO synthesis in the impaired production of maspin in human breast cancer. *J. Cancer Res. Clin. Oncol. 132*, 389−398.

(13) Bhattacharya, S., Chakrabortypatra, S., Basuroy, S., Kahn, N. N., and Sinha, A. K. (2001) Purification and properties of insulin-activated nitric oxide synthase from human erythrocyte membranes. *Arch. Physiol. Biochem. 109*, 441−449.

(14) Forstermann, U., Mulsch, A., Bohme, E., and Busse, R. (1986) Stimulation of soluble guanylate cyclase by an acetylcholine-induced endothelium-derived factor from rabbit and canine arteries. *Circ. Res. 58*, 531−538.
(15) Kahn, N. N., Acharya, K., Bhattacharya, S., Acharya, R., Mazumder, S., Bauman, W. A., and Sinha, A. K. (2000) Nitric oxide: The "second messenger" of insulin. *IUBMB Life 49*, 441−450.
(16) Busch, T., Bartsch, P., Pappert, D., Grunig, E., Hildebrandt, W., Elser, H., Falke, K. J., and Swenson, E. R. (2001) Hypoxia decreases exhaled nitric oxide in mountaineers susceptible to high-altitude pulmonary edema. *Am. J. Respir. Crit. Care Med. 163*, 368−373.
(17) Nakchbandi, I. A., Inzucchi, S. E., and Wirth, J. A. (2000) Prognostic Value of von Willebrand Factor Concentrations in Pulmonary Hypertension. *Chest 118*, 1225−1226.
(18) Frankel, D. S., Meigs, J. B., Massaro, J. M., Wilson, P. W., O'Donnell, C. J., D'Agostino, R. B., and Tofler, G. H. (2008) Von Willebrand factor, type 2 diabetes mellitus, and risk of cardiovascular disease: The Framingham offspring study. *Circulation 118*, 2533−2539.
(19) Chambers, D. C., Boldy, D. A., and Ayres, J. G. (1999) Chronic respiratory symptoms, von Willebrand factor and longitudinal decline in FEV1. *Respir. Med. 93*, 726−733.
(20) Khan, G., Biswas, I., Garg, I., Singh, B., and Agrawala, P. K. (2011) Hypobaric hypoxia induces hypercoagulable state: Role of inflamation and endothelial dysfunction. In *XXIII Congress of the International Society on Thrombosis and Haemostasis*, S2 edition, pp 618, Wiley, Kyoto, Japan.
(21) Pinsky, D. J., Naka, Y., Liao, H., Oz, M. C., Wagner, D. D., Mayadas, T. N., Johnson, R. C., Hynes, R. O., Heath, M., Lawson, C. A., and Stern, D. M. (1996) Hypoxia-induced exocytosis of endothelial cell Weibel-Palade bodies. A mechanism for rapid neutrophil recruitment after cardiac preservation. *J. Clin. Invest. 97*, 493−500.
(22) Biswas, I., Garg, I., Singh, B., and Khan, G. A. (2012) A key role of toll-like receptor 3 in tissue factor activation through extracellular signal regulated kinase 1/2 pathway in a murine hypoxia model. *Blood Cells, Mol., Dis. 49*, 92−101.
(23) Jia, L., Bonaventura, C., Bonaventura, J., and Stamler, J. S. (1996) S-Nitrosohaemoglobin: A dynamic activity of blood involved in vascular control. *Nature 380*, 221−226.
(24) Cox, R. D., and Frank, C. W. (1982) Determination of nitrate and nitrite in blood and urine by chemiluminescence. *J. Anal. Toxicol. 6*, 148−152.
(25) Engvall, E., and Perlmann, P. (1972) Enzyme-linked immunosorbent assay, Elisa. 3. Quantitation of specific antibodies by enzyme-labeled anti-immunoglobulin in antigen-coated tubes. *J. Immunol. 109*, 129−135.
(26) Mihov, D., Vogel, J., Gassmann, M., and Bogdanova, A. (2009) Erythropoietin activates nitric oxide synthase in murine erythrocytes. *Am. J. Physiol. 297*, C378−C388.
(27) Khan, G. A., Girish, G. V., Lala, N., Di Guglielmo, G. M., and Lala, P. K. (2011) Decorin is a novel VEGFR-2-binding antagonist for the human extravillous trophoblast. *Mol. Endocrinol. 25*, 1431−1443.
(28) Furlan, M., Robles, R., Affolter, D., Meyer, D., Baillod, P., and Lammle, B. (1993) Triplet structure of von Willebrand factor reflects proteolytic degradation of high molecular weight multimers. *Proc. Natl. Acad. Sci. U.S.A. 90*, 7503−7507.
(29) Otta, A. (1968) Excitation of surface plasma waves in silver by the method of frustrated total reflection. *J. Physiol. 216*, 398−410.
(30) Kretschmann, E., and Raether, H. (1968) Radiative decay of non-radiative surface plasmons excited by light. *Z. Naturforsch. 23*, 2135−2136.
(31) Nylander, C., Leidgerg, B., and Lind, T. (1982) Gas-detection by means of surface-plasmon resonance. *Sens. Actuators 3*, 79−88.
(32) Matthews, D. R., Hosker, J. P., Rudenski, A. S., Naylor, B. A., Treacher, D. F., and Turner, R. C. (1985) Homeostasis model assessment: Insulin resistance and $\beta$-cell function from fasting plasma glucose and insulin concentrations in man. *Diabetologia 28*, 412−419.
(33) Lemini, C., Rubio-Poo, C., Silva, G., Garcia-Mondragon, J., Zavala, E., Mendoza-Patino, N., Castro, D., Cruz-Almanza, R., and Mandoki, J. J. (1993) Anticoagulant and estrogenic effects of two new 17$\beta$-aminoestrogens, butolame [17$\beta$-(4-hydroxy-1-butylamino)-1,3,5(10)-estratrien-3-ol] and pentolame [17$\beta$-(5-hydroxy-1-pentylamino)-1,3,5(10)-estratrien-3-ol]. *Steroids 58*, 457−461.
(34) Dejana, E., Callioni, A., Quintana, A., and de Gaetano, G. (1979) Bleeding time in laboratory animals. II. A comparison of different assay conditions in rats. *Thromb. Res. 15*, 191−197.
(35) Murata, T., Sato, K., Hori, M., and Kahari, H. (2002) Decreased endothelial nitric-oxide synthase (eNOS) activity resulting from abnormal interaction between eNOS and its regulatory proteins in hypoxia-induced pulmonary hypertension. *J. Biol. Chem. 277*, 144085−144092.
(36) Gao, S., Chen, J., Brodsky, S. V., Huang, H., Adler, S., Lee, J. H., Dhadwal, N., Cohen-Gould, L., Gross, S. S., and Goligorsky, M. S. (2004) Docking of endothelial nitric oxide synthase (eNOS) to the mitochondrial outer membrane: A pentabasic amino acid sequence in the autoinhibitory domain of eNOS targets a proteinase K-cleavable peptide on the cytoplasmic face of mitochondria. *J. Biol. Chem. 279*, 15968−15974.
(37) Sowa, G., Liu, J., Papapetropoulos, A., Rex-Haffner, M., Hughes, T. E., and Sessa, W. C. (1999) Trafficking of endothelial nitric-oxide synthase in living cells. Quantitative evidence supporting the role of palmitoylation as a kinetic trapping mechanism limiting membrane diffusion. *J. Biol. Chem. 274*, 22524−22531.
(38) Punjabi, N. M., Shahar, E., Redline, S., Gottlieb, D. J., Givelber, R., and Resnick, H. E. (2004) Sleep-disordered breathing, glucose intolerance, and insulin resistance: The Sleep Heart Health Study. *Am. J. Epidemiol. 160*, 521−530.
(39) Lee, E. J., Alonso, L. C., Stefanovski, D., Strollo, H. C., Romano, L. C., Zou, B., Singamsetty, S., Yester, K. A., Mcgaffin, K. R., Garcia-Ocana, A., and O'Donnell, C. P. (2013) Time-dependent changes in glucose and insulin regulation during intermittent hypoxia and continuous hypoxia. *Eur. J. Appl. Phyiol. 113*, 467−468.
(40) Peltonen, G. L., Scalzo, R. L., Schweder, M. M., Larson, D. G., Luckasen, G. J., Irwin, D., Hamilton, K. L., Schroeder, T., and Bell, C. (2012) Sympathetic inhibition attenuates hypoxia induced insulin resistance in healthy adult humans. *J. Physiol. 590*, 2801−2809.
(41) Gamboa, J. L., Garcia-Cazarin, M. L., and Andrade, F. H. (2011) Chronic hypoxia increases insulin-stimulated glucose uptake in mouse soletus muscle. *Am. J. Physiol. 300*, R85−R91.
(42) Bonow, R. O. (2002) Primary prevention of cardiovascular disease: A call to action. *Circulation 106*, 3140−3141.
(43) Natali, A., Toschi, E., Baldeweg, S., Ciociaro, D., Favilla, S., Sacca, L., and Ferrannini, E. (2006) Clustering of insulin resistance with vascular dysfunction and low-grade inflammation in type 2 diabetes. *Diabetes 55*, 1133−1140.
(44) Ip, M. S., Lam, B., Chan, L. Y., Zheng, L., Tsang, K. W., Fung, P. C., and Lam, W. K. (2000) Circulating nitric oxide is suppressed in obstructive sleep apnea and is reversed by nasal continuous positive airway pressure. *Am. J. Respir. Crit. Care Med. 162*, 2166−2171.
(45) Iwase, H., Kobayashi, M., Nakajima, M., and Takatori, T. (2001) The ratio of insulin to C-peptide can be used to make a forensic diagnosis of exogenous insulin overdosage. *Forensic Sci. Int. 115*, 123−127.
(46) Djamiatun, K., van der Ven, A. J., de Groot, P. G., Faradz, S. M., Hapsari, D., Dolmans, W. M., Sebastian, S., Fijnheer, R., and de Mast, Q. (2012) Severe dengue is associated with consumption of von Willebrand factor and its cleaving enzyme ADAMTS-13. *PLoS Neglected Trop. Dis. 6*, e1628.
(47) Young, M. E., Radda, G. K., and Leighton, B. (1997) Nitric oxide stimulates glucose transport and metabolism in rat skeletal muscle in vitro. *Biochem. J. 322* (Part1), 223−228.
(48) Chakraborty, K., Khan, G. A., Banerjee, P., Ray, U., and Sinha, A. K. (2003) Inhibition of human blood platelet aggregation and the stimulation of nitric oxide synthesis by aspirin. *Platelets 14*, 421−427.
(49) McConell, G. K., and Kingwell, B. A. (2006) Does nitric oxide regulate skeletal muscle glucose uptake during exercise? *Exercise Sport Sci. Rev. 34*, 36−41.